DOI:10.1002/ejic.201402117

Hierarchical Self-Assembly of Luminescent Eu^{III} Complexes on Silicon

Kasjan Misztal,[a] Cristina Tudisco,[b] Andrea Sartori,[a][‡] Joanna M. Malicka,[c][‡‡] Riccardo Castelli,[a][‡] Guglielmo G. Condorelli,[b] and Enrico Dalcanale*[a]

Keywords: Supramolecular chemistry / Host–guest systems / Cavitands / Self-assembly / Lanthanides / Luminescence / Silicon

We have combined the metal-coordinating features of phenanthroline with the remarkable complexing properties of tetraphosphonate (Tiiii) cavitands towards *N*-methylammonium salts with the aim of assembling novel luminescent ternary complexes. The formation of such complexes was first tested in solution: the charged sarcosine derivative **1**, bearing a phenanthroline moiety, was complexed by the cavitand Tiiii-**A**, followed by coordination of Eu^{III}–tris(β-diketonate) complex **2**. The occurrence of the self-assembly has been proven by NMR spectroscopy, mass spectrometry and photophysical measurements. The transfer of this binding protocol to the surface showed the complete orthogonality of these interactions, as verified by control experiments on complexation-inactive surfaces. The formation of the ternary complexes on the silicon surface was monitored by means of X-ray photoelectron spectroscopy and luminescence spectroscopy. The emission properties of the silicon-bound Si-Tiiii-**B·1·2** and the corresponding ternary complex Tiiii-**A·1·2** in solution are similar, which indicates that the transfer of the self-assembly process onto silicon does not significantly perturb the Eu^{III} coordination environment. The self-assembly protocol illustrated here can be extended to a wide variety of lanthanide ions and can be implemented for applications in sensing, bioimaging and optoelectronic devices.

Introduction

The formation of hierarchical monolayers and multilayers on different surfaces by exploiting supramolecular interactions represents a theme of great interest in contemporary chemistry.[1,2] The idea behind this approach is to use the thermodynamic control and reversibility of noncovalent interactions for the error-free generation of specific architectures directly on surfaces.[3] A substantial contribution to the self-assembly protocols for 2D and 3D structures was given by the development of molecular-recognition schemes on surfaces,[4] which tapped into the large body of available synthetic receptors that have been designed, prepared and tested over the last three decades. Among them, cavitands[5] are particularly versatile systems, the complexation ability of which has been exploited not only for the recognition of target molecules[6] but also for the fabrication of well-defined 2D and 3D molecular assemblies.[7] Some examples of cavitand-decorated surfaces of gold[8] and silicon[9] in which the molecular-recognition properties of cavitands have been exploited for the precise fabrication of a specific molecular structure have been reported. Recently, β-cyclodextrins were employed as molecular receptors for the self-assembly of Eu^{III} luminescent complexes on glass.[10] The antenna sensitizer and the Eu complex were independently anchored on the glass surface through hydrophobic adamantyl–cyclodextrin complexation by using a multivalency approach. The two components interact on the surface, thus producing localized sensitized emission.

In the present work, we describe an alternative, sequential self-assembly protocol aimed at building Eu^{III} luminescent coordination structures on silicon. Our approach is based on the combination of the molecular-recognition properties of a tetraphosphonate cavitand with the metal-coordination ability of specific guests.

Eu^{III} and Tb^{III} complexes display exceptional photophysical properties[11] such as high photoluminescence quantum yield (PLQY) in the visible spectral region, long excited-state lifetimes, large Stokes shifts and sharp emission profiles related to f–f electronic transitions. The char-

---

[a] Dipartimento di Chimica and INSTM UdR di Parma,
University of Parma,
Parco Area delle Scienze 17/A, 43124 Parma, Italy
E-mail: enrico.dalcanale@unipr.it
http://www.dalcanalegroup.it
[b] Dipartimento di Scienze Chimiche and INSTM UdR di Catania, University of Catania, ISTM-CNR,
V.le A. Doria 6, 95125 Catania, Italy
[c] Molecular Photoscience Group, Istituto per la Sintesi Organica e la Fotoreattività del CNR (ISOF-CNR),
Via P. Gobetti 101, 40129 Bologna, Italy
[‡] Current address: Dipartimento di Farmacia, University of Parma,
Parco Area delle Scienze 27A, 43124 Parma, Italy
[‡‡] Current address: Consorzio MIST E-R, Via P. Gobetti 101, 40129 Bologna, Italy

Supporting information for this article is available on the WWW under http://dx.doi.org/10.1002/ejic.201402117.

acteristic red and green photoluminescence of trivalent Eu and Tb ions,[12] upon ultraviolet-light irradiation, has been exploited from the fundamental and applicative point of view. Accordingly, materials based on Eu^{III} and Tb^{III} are extensively utilized in light-conversion molecular devices, as phosphors in lighting technologies, as well as for sensing purposes and memory devices.[13,14] Although some examples of Eu^{III} complexes covalently attached on surfaces have been reported,[15,16] to the best of our knowledge no examples of noncovalent self-assembly of lanthanide luminescent probes on silicon surfaces have been described in the literature.

The main goal of the present work is the development of a strategy for the precise and reversible hierarchical assembly on silicon of a luminescent Eu^{III} complex, which is bound to a surface-anchored cavitand by means of a sarcosine moiety bearing a phenanthroline ligand. The design of the connecting ligand was determined by the following experimental observations: (i) the high association constant of sarcosine with tetraphosphonate cavitands,[17] and (ii) the well-known ability of phenanthroline[18,19] to serve as a strong bidentate ligand and efficient sensitizer for Eu^{III}–β-diketonates.

Results and Discussion

Design and Strategy

The compounds used in the present work are shown in Scheme 1. The precise and reversible hierarchical assembly on silicon was obtained by using host–guest interactions and metal–ligand coordination in sequence. This multistep approach involves the recognition process of tetraphosphonate cavitands (Tiiii)[20] anchored on the silicon surfaces towards a sarcosine unit[17] connected to a phenanthroline ligand (**1**), followed by the coordination of **1** with the europium β-diketonate complex **2** used as the luminescent probe. The related nonluminescent and diamagnetic yttrium β-diketonate **3** was chosen as the reference compound for the NMR spectroscopic characterization in solution and for photophysical control experiments on the surface. Cavitand-decorated silicon surfaces were prepared by photochemical grafting.[21] The entire process was fully tested in solution, and then successfully transferred to the solid state where it was monitored by means of X-ray photoelectron spectroscopy (XPS) and luminescence spectroscopy.

Self-Assembly in Solution

The formation of ternary complexes was first carried out in solution to prove its feasibility (Figure 1). The first step was the complexation of the methylammonium guest **1** inside the Tiiii[C_3H_7, CH_3, Ph] (hereafter referred to as Tiiii-**A**) cavity in methanol, monitored by ^{31}P and ^{1}H NMR spectroscopy measurements. Figure S1 in the Supporting Information shows the ^{1}H NMR spectrum of the host–guest complex formed by **1** and Tiiii-**A** (Tiiii-**A·1**). Diagnostic upfield shifts of the guest signals were observed, as expected for hosted species that experience the shielding effect of the cavity.[17] In particular, the signals of the *N*-CH_3 moiety moved over 3 ppm upfield to $\delta = -0.53$ ppm; other resonances attributed to the sarcosine moiety as well as to the phenanthroline unit were also shifted. The ^{31}P resonance of the four P=O groups moved downfield by almost 5 ppm (from $\delta = 5.9$ to 10.8 ppm; Figure S2 in the Supporting Information). The upfield shift of the methyl residue is diagnostic of *N*-CH_3 inclusion into the cavity, whereas the downfield shift of P=O signals is a clear indication of the

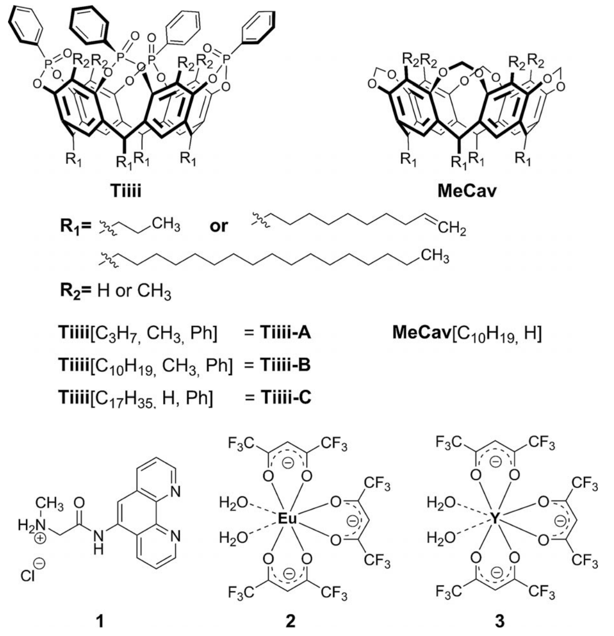

Scheme 1. Molecular structures of the compounds used in the present work.

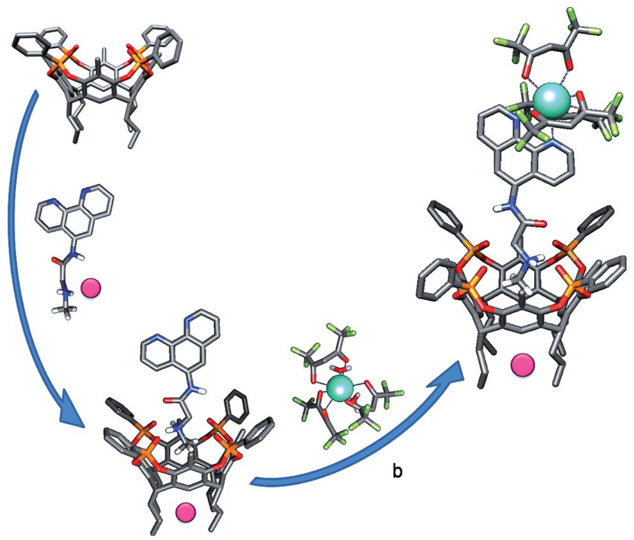

Figure 1. Ternary complex formation in solution (10 mM of each component): (a) host–guest Tiiii-**A·1** complex formation in methanol; (b) coordination between Tiiii-**A·1** and **2** (or **3**) in dichloromethane. The pink ball represents the chloride anion of the ammonium-based ligand **1**.

participation of phosphonates in the complexation of the guest.

The ternary complexes between Tiiii-**A**·**1** and the metal precursors **2** or **3** were formed quantitatively by simply mixing the three components in dichloromethane. The formation of Tiiii-**A**·**1**·**3** was monitored by means of ^{1}H and ^{31}P NMR spectroscopy. In the proton spectrum of Tiiii-**A**·**1**·**3** the downfield shift of the peaks belonging to the phenanthroline was observed, which is diagnostic of the metal complexation (Figure S1 in the Supporting Information). The phosphorus peak remained almost unchanged, which indicated that the metal ion does not compete with sarcosine for the cavity. Because of the paramagnetic properties of Eu^{III}, ^{1}H NMR spectroscopy was not used to monitor the formation of the Tiiii-**A**·**1**·**2** complex, whereas the phosphorus spectrum is similar to that of the diamagnetic yttrium derivative Tiiii-**A**·**1**·**3** (Figure S3 in the Supporting Information), so it is safe to assume that the Tiiii-**A**·**1**·**2** complex was formed. The self-assembly outcome changes dramatically by replacing **1** with bare phenanthroline: Tiiii-**A** substitutes phenanthroline in the coordination sphere of Y^{III}, as indicated by a downfield shift in the ^{31}P NMR spectrum (Figure S11 in the Supporting Information). Therefore, the higher affinity of sarcosine for the cavity shifts the equilibrium toward the exclusive formation of the ternary complex Tiiii-**A**·**1**·**2**. Unfortunately, we have been unable to precisely establish the coordination mode of Tiiii with Ln^{III}. The presence of ternary species was also confirmed by high-resolution mass spectrometry (HRMS). The HRMS spectrum of the analogous complex Tiiii-**C**·**1**·**2** in acetonitrile, in which the cavitand has a longer alkyl chain at the lower rim, exhibited a peak at *m*/*z* corresponding to the complex without the chloride anion (Figure S4 in the Supporting Information).

Absorption and Luminescence Spectra in Solution

The formation of the hierarchical complexes Tiiii-**A**·**1**·**2** and Tiiii-**A**·**1**·**3** is further supported by photophysical investigations. The UV/Vis absorption spectrum of **2** in dichloromethane spans across the range 260–350 nm with a maximum centred at 290 nm (Figure S5 in the Supporting Information). The phenanthroline ligand **1** absorbs in the same spectral range but its maximum is located at higher energies (275 nm; Figure S5). In line with these findings, the absorption spectrum of the compound obtained from the phenanthroline system **1** and the Eu–β-diketonate complex **2** (**1**·**2**) is the sum of the spectral features of its building blocks and shows a maximum at 285 nm (Figure S5). The absorption spectrum of the analogous yttrium–β-diketonate complex **1**·**3** is virtually identical to that of **1**·**2**, which indicates the same electronic transitions in both compounds, as expected (Figure S6 in the Supporting Information). The Tiiii-**A** cavitand does not absorb light beyond 290 nm, and the formation of Tiiii-**A**·**1**·**2** leads only to a broadening of the absorption band (Figure S5). Absorption spectra of **1**·**2**, **1**·**3**, Tiiii-**A**, and Tiiii-**A**·**1** are presented in Figure S7 in the Supporting Information.

All the investigated europium compounds, **2**, **1**·**2** and Tiiii-**A**·**1**·**2**, exhibit characteristic Eu^{III} emission bands due to the f–f transitions (Figure 2). The emission spectra consist of $^5D_0 \rightarrow {}^7F_J$ transitions (J = 0–4) mainly dominated by the $^5D_0 \rightarrow {}^7F_1$ and $^5D_0 \rightarrow {}^7F_2$ sharp emission bands centred at 590 and 612 nm, respectively. The perfect overlapping of the emission spectra between **2**, **1**·**2** and Tiiii-**A**·**1**·**2** complexes shows that the coordination sphere of the europium cation remains virtually unchanged after encapsulation in the cavity. Notably, the PLQY of **2** is 15.5%, and increases to 25.9% for **1**·**2**. In the latter, the phenanthroline ligand fills the coordination sphere around the europium cation and eliminates vibrational quenching from water molecules and also serves as a light-harvesting antenna. PLQY of the ternary complex Tiiii-**A**·**1**·**2** in solution is 20.0%, which is intermediate between those of **2** and **1**·**2**. The trend of the lifetimes values is in perfect agreement with that observed for the quantum yields (Table 1).

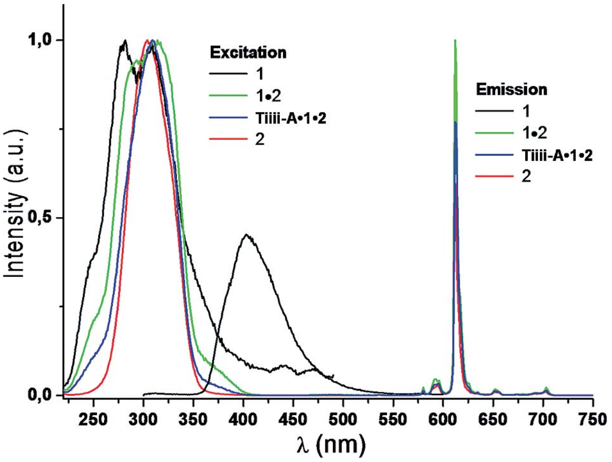

Figure 2. Emission and excitation spectra of the compounds in dichloromethane at 298 K. Excitation spectra: λ_{em} = 612 nm in all cases but **1** for which λ_{em} = 410 nm; emission spectra: λ_{ex} = 280 nm.

Table 1. Photophysical data of solutions of the compounds in dichloromethane at 298 K.

	PLQY [%]	Excited-state lifetime
1	5.7	4.90 ns[b]
2	15.5	0.75 ms[a]
1·**2**	25.9	0.85 ms[a]
Tiiii-**A**·**1**·**2**	20.0	0.80 ms[a]
Tiiii-**A**·**1**	2.7	3.70 ns[b]
1·**3**	1.9	3.10 ns[b]
Tiiii-**A**·**1**·**3**	1.7	3.50 ns[b]

[a] Eu^{III}-centred luminescence. [b] Phenanthroline-centred fluorescence.

Y^{III} complexes (**1**·**3** and Tiiii-**A**·**1**·**3**) do not exhibit metal-centred emission due to the closed-shell configuration of the ion. Therefore they were investigated as reference compounds. The only luminescence band observed was that of the sarcosine–phenanthroline ligand **1** at λ_{max} = 440 nm. The emission profile of **1** in Tiiii-**A**·**1**·**3** matches well with the emission of the ligand in Tiiii-**A**·**1** and is shifted towards longer wavelengths relative to free **1** (λ_{max} = 290 nm) owing

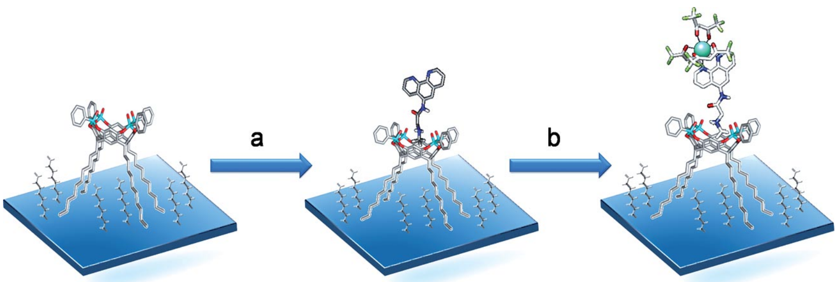

Figure 3. Si-Tiiii-**B** hierarchical self-assembly protocol with (a) guest **1** and (b) subsequently with metal complexes **2** or **3**.

to the confinement effect of the cavitand. PLQY of free ligand **1** was 5.7%. This value decreases to 2.7% in Tiiii-**A**, which suggests the presence of some electronic interaction between the phenanthroline moiety and the cavitand. In the case of the metal complex **1·3**, the PLQY is decreased to 1.9%. The difference relative to free **1** suggests the presence of some electronic perturbation induced by the yttrium cation.

Self-Assembly on the Tiiii-Functionalized Si Surface

The noncovalent anchoring on the silicon surface is schematically illustrated in Figure 3. The preliminary step was the preparation of the Tiiii-**B**-functionalized Si surface (Si-Tiiii-**B**) by covalent grafting of a mixed Tiiii-**B**/1-octene monolayer, by means of photochemical hydrosilylation. According to previous studies,[9b,21] the use of 1-octene as a spectator spacer in the mixed monolayers improves the passivation of the Si surface, thus minimizing substrate oxidation due to aging. XPS measurements of the grafted surfaces showed the typical P 2p band of the silicon-anchored Tiiii cavitand. The detailed characterization of the Si-Tiiii-**B** surface is reported elsewhere.[9b]

The self-assembly protocol implemented in solution was then transferred to the silicon surface (Figure 3). The first step was the binding of **1** on the Si-grafted cavitand through the complexation of the methyl ammonium moiety. This was accomplished by dipping Si-Tiiii-**B** in a 1 mM solution of **1** in methanol. The surface functionalized with the host–guest adduct (Si-Tiiii-**B·1**) was then dipped in a 1 mM solution of **2** (or **3**) in THF to bind the metal complex through coordination with the phenanthroline moiety to yield Si-Tiiii-**B·1·2** (or Si-Tiiii-**B·1·3**, respectively).

Step-by-Step Monitoring of the Self-Assembly Process

Each self-assembly step was monitored by XPS. The atomic compositions of Si-Tiiii-**B**, Si-Tiiii-**B·1**, Si-Tiiii-**B·1·2** and Si-Tiiii-**B·1·3** are reported in Table 2. A low N 1s signal was already present in the Si-Tiiii-**B** sample owing to adventitious N-containing species. However, after treatment with guest **1**, a significant increase of the N 1s signal was observed. In addition, the shape of the XPS N 1s band (Figure 4) is consistent with the molecular formula of **1**. In fact, the band consists of two components: (i) a main feature at 400.0 eV assigned to the two phenanthroline nitrogen atoms and the nitrogen atoms of the amidic bond (N_{lig}), and (ii) a less intense component at 402.0 eV assigned to the protonated nitrogen of sarcosine (N_{sar}). The observed intensity ratio N_{lig}/N_{sar} is about 3:1 as expected from the molecular structure. The successful coordination affording Si-Tiiii-**B·1·2** and Si-Tiiii-**B·1·3**, respectively, was corroborated by the presence of Eu (or Y) XPS bands together with the F 1s signal due to the coordinated β-diketonate ligands (Table 2).

Table 2. Elemental composition data from XPS measurements for selected surfaces.

	Atomic fractions [%]							
	P	Si	O	C	N	F	Eu	Y
Si-Tiiii-**B**	1.1	16.3	31.9	50.4	0.3	–	–	–
Si-Tiiii-**B·1**	1.0	12.9	30.5	53.9	1.7	–	–	–
Si-Tiiii-**B·1·2**	0.9	12.2	28.8	49.3	1.2	6.9	0.38	–
Si-Tiiii-**B·1·3**	0.9	11.1	21.3	59.9	1.1	5.4	–	0.32
Si-MeCav**·1·2**	–	19.9	26.9	52.4	0.3	0.5	<0.03	–

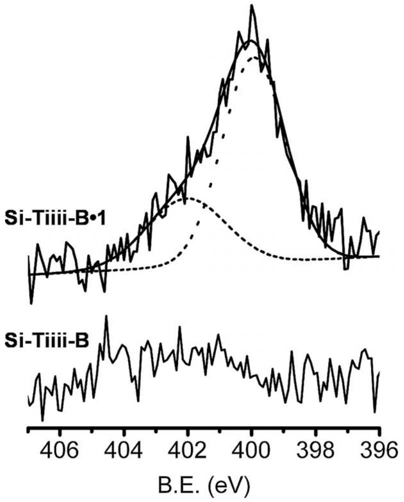

Figure 4. High-resolution N 1s XPS region of Si-Tiiii-**B** and Si-Tiiii-**B·1**.

The Eu 3d XPS region of the Si-Tiiii-**B·1·2** sample shows the characteristic doublet of Eu $3d_{5/2}$ and Eu $3d_{3/2}$ that is centred at 1135.1 and 1164.8 eV, respectively; this is consistent with the presence of Eu^{III} (Figure 5, a).[16] It is worth noting that a low-intensity doublet is observed at 1125.1 and 1155.1 eV, which could indicate the presence of reduced

Eu^{II}.[22] The relative intensity of these bands (with respect to the main doublet) increases with X-ray irradiation time and the amount of Eu^{II} is negligible for very short XPS acquisition times (Figure S8 in the Supporting Information). This suggests that europium is present only as Eu^{III} in the monolayer and that reduction is produced during the XPS analysis. In the Si-Tiiii-**B·1·3** sample, Y $3d_{5/2}$ and Y $3d_{3/2}$ peaks (Figure 5, b) appear at 158.8 and 160.6 eV, respectively, consistent with the presence of a Y^{III} compound.

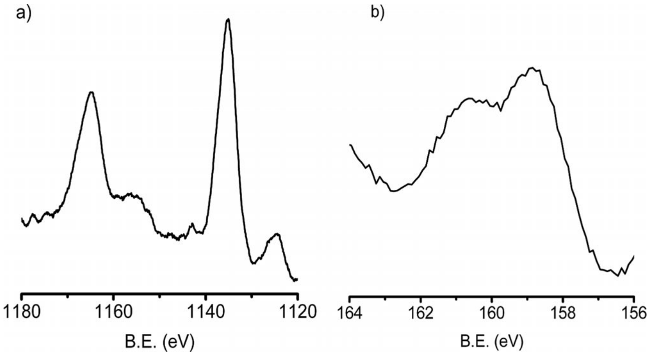

Figure 5. High-resolution XPS regions of (a) Eu 3d of Si-Tiiii-**B·1·2** and (b) Y 3d of Si-Tiiii-**B·1·3**.

To demonstrate that the self-assembly on the surface is driven by the molecular-recognition properties of the Tiiii-**B** cavity and to rule out any physisorption phenomena of the metal complexes on the surface, a specific control experiment has been designed and executed. A blank sample made of a complexation-inactive methylene-bridged cavitand grafted on silicon (Si-MeCav) was prepared. The resulting Si-MeCav surface was treated with guests **1** and **2** (Si-MeCav·**1·2**) similarly to Si-Tiiii-**B·1·2**. XPS analysis of Si-MeCav·**1·2** (Table 2) did not show significant amounts of nitrogen, europium or fluorine, which shows that physisorption on the surface is negligible, and the complexation capability of the Tiiii-**B** cavity is a key requirement for the self-assembly process.

The atomic ratios Eu/N/F and Y/N/F of Si-Tiiii-**B**·**1**·**2** and Si-Tiiii-**B**·**1**·**3** are 1:3.2:18.2 and 1:3.4:16.9, respectively. They are close to the theoretical expected ratio 1:4:18, although a slightly lower amount of N is observed in both cases. This behaviour can be due to a direct coordination of the metal complexes in the Tiiii-**B** cavity, to a very limited extent. To investigate this possible side-reaction pathway, Si-Tiiii-**B** surfaces without guest **1** were treated with **2** and **3**. XPS analyses of the samples thus obtained (Si-Tiiii-**B**·**2** and Si-Tiiii-**B**·**3**) showed the presence of the metals and fluorine in amounts comparable to that of Si-Tiiii-**B**·**1**·**2** and Si-Tiiii-**B**·**1**·**3** (Figures S9 and S10, respectively, in the Supporting Information), which indicated that the Tiiii-**B** cavity can interact directly with complex **2** or **3**. However, obtained (Table S1 in the Supporting Information) Eu/F and Y/F atomic ratios (1:7 and 1:8, respectively) are different from the theoretical value (1:18) expected for intact complexes. This behaviour suggests that the direct complexation of **2** and **3** on the cavitand-decorated surface does not preserve the original metal-coordination environment, but induces ligand dissociation.

Photophysical Measurements on the Surface

To evaluate the presence of the free or uncomplexed phenanthroline ligand in the self-assembled systems, the luminescence properties of Si-Tiiii-**B·1**, Si-Tiiii-**B·1·2**, Si-Tiiii-**B·1·3** and Si-Tiiii-**B·2** surfaces have been examined in the spectral window of the phenanthroline fluorescence band (λ_{ex} = 270 nm; Figure 6) for the various surfaces. Only Si-Tiiii-**B·1** showed the band of the phenanthroline ligand (λ_{max} = 440 nm), whereas in all the other samples no luminescence was detected (Figure 6). For Si-Tiiii-**B·2** this result is obvious, since phenanthroline is not present on the surface. However, in the case of Si-Tiiii-**B·1·2** the absence of phenanthroline emission corroborates the occurrence of the energy-transfer properties of the Eu^{III} ion.

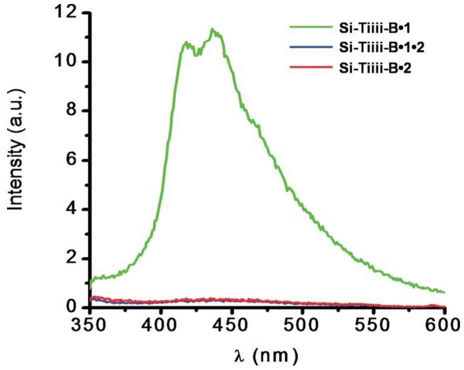

Figure 6. Emission spectra of different surfaces in the spectral window of the phenanthroline fluorescence.

Eu^{III} emission was evaluated in the 480–750 nm range (λ_{ex} = 320 nm) for both the Si-Tiiii-**B·1·2** and Si-Tiiii-**B·2** surfaces. Si-Tiiii-**B·1·2** exhibits emission bands related to $^5D_0 \rightarrow {}^7F_1$, $^5D_0 \rightarrow {}^7F_2$, $^5D_0 \rightarrow {}^7F_3$ and $^5D_0 \rightarrow {}^7F_4$ transitions, at 592, 610, 648 and 690 nm, respectively, shifted a few nanometres towards higher energies relative to the compound in solution. For Si-Tiiii-**B·2** only the strong signals of $^5D_0 \rightarrow {}^7F_1$ and $^5D_0 \rightarrow {}^7F_2$ were observed (Figure 7). The

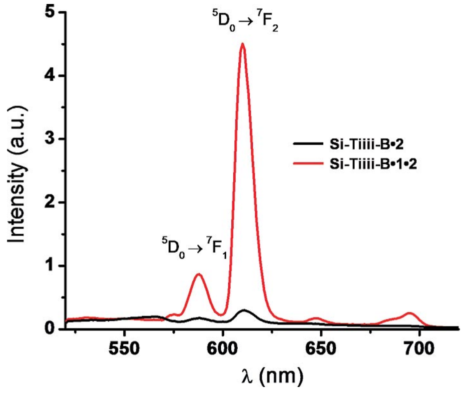

Figure 7. Fluorescence spectra of Si-Tiiii-**B·1·2** (red trace) and Si-Tiiii-**B·2** (black trace) surfaces probed at five different points of the samples; λ_{ex} = 320 nm.

emission intensity recorded for the Si-Tiiii-**B**·**1**·**2** surfaces is significantly higher than that of Si-Tiiii-**B**·**2**, thanks to the sensitizing properties of the phenanthroline towards Eu^{III}, which ultimately improves light absorption and, accordingly, emission output. Moreover, the relative intensities of the $^5D_0 \rightarrow {}^7F_1$ and $^5D_0 \rightarrow {}^7F_2$ transitions are different for the two surfaces. In particular, for Si-Tiiii-**B**·**1**·**2** the intensity ratio between the $^5D_0 \rightarrow {}^7F_1$ and $^5D_0 \rightarrow {}^7F_2$ transitions (1:4) is similar to that in solution (1:5), whereas for Si-Tiiii-**B**·**2** it is remarkably different (1:2). These results suggest that the self-assembly process in the presence of **1** occurs without significant changes of the Eu coordination environment relative to that of the solution process. By contrast, the direct complexation of **2** in the Tiiii cavity leads to a significant modification of the original Eu environment.

Finally, no emission was observed for Si-MeCav·**1**·**2**. This result matches with XPS findings, which indicates that no Eu^{III} complex was anchored on the surface in the absence of specific Tiiii receptors.

Conclusion

Herein, we have reported the first example of the hierarchical self-assembly of luminescent lanthanide complexes on silicon. Formation of these supramolecular structures on a Si surface has been confirmed by two independent analytical techniques (XPS and fluorescence) and validated by control experiments with surfaces decorated with a complexation-inactive methylene-bridged cavitand. Self-assembly on the cavitand-functionalized surface with a sarcosine–phenanthroline ligand followed by [Eu(hfac)$_3$] (hfac = hexafluoroacetylacetonate) coordination afforded a more strongly emitting surface than direct coordination of [Eu(hfac)$_3$] by Tiiii due to the sensitization of the Eu^{III} ion by the phenanthroline ligand. The present approach can be implemented for applications in sensing, bioimaging and optoelectronic devices. The use of the universal bidentate ligand **1** allows the complexation of other lanthanide ions, as well as of metals in general. Moreover, the self-assembly of these ternary complexes on silicon will widen the spectrum of possible applications, since silicon is a technologically important inorganic platform.

Experimental Section

General: All commercial reagents were ACS reagent grade and used as received. Solvents were dried and distilled by using standard procedures. ^{1}H NMR spectra were recorded on Bruker Avance 400 (400 MHz) and Bruker Avance 300 (300 MHz) NMR spectrometers. All chemical shifts (δ) were reported in parts per million (ppm) relative to proton resonances resulting from incomplete deuteration of NMR spectroscopy solvents. ESI-MS experiments were performed on a Waters ZMD spectrometer equipped with an electrospray interface. The exact mass values were determined using a LTQ ORBITRAP XL Thermo spectrometer equipped with an electrospray interface. This section only includes the synthesis and characterization of ligand **1** from commercially available 5-amino-1,10-phenanthroline (**5**), through a modified literature procedure[14] and self-assembly in solution and on a silicon surface; syntheses of tetraphosphonate cavitands Tiiii-**A**[23] and Tiiii-**B** without the methyl groups at the upper rim.[24] The NMR and MS spectra of the formation of complexes can be found in the Supporting Information.

Bromo-*N*-(1,10-phenanthrolin-5-yl)acetamide (4): 5-Amino-1,10-phenanthroline (0.20 g, 1.03 mmol) was placed in a round-bottomed flask under argon. Acetonitrile (dry, 40 mL) and triethylamine (0.11 g, 1.04 mmol, 0.15 mL) were added and the suspension was stirred for 30 min at room temperature. The mixture was cooled to 0 °C before bromoacetylchloride (0.19 g, 1.23 mmol, 0.10 mL, 1.2 equiv.) in acetonitrile (5 mL) was added dropwise. The mixture was left stirring for 16 h at room temperature and analysis by TLC [CH_2Cl_2/MeOH(saturated with NH_3) 9:1] showed no further progress of the reaction. The solvent was removed under reduced pressure and the residue was solubilized in 5% K_2CO_3 aqueous solution (10 mL). Triple extraction with dichloromethane was conducted and organic layers were collected and evaporated, yielding a brown residue (0.25 g) that was next purified by silica column chromatography using 95:5 CH_2Cl_2/MeOH(NH_3) as eluent to give a pale brown solid (0.166 g, 51%). ^{1}H NMR (400 MHz, $CDCl_3$, 298 K): δ = 9.26 (d, J = 4.2 Hz, 1 H), 9.18 (d, J = 5.6 Hz, 1 H), 8.81 (br. s, 1 H, NH), 8.39 (s, 1 H), 8.36 (d, J = 8.5 Hz, 1 H), 8.27 (d, J = 8.0 Hz, 1 H), 7.74 (dd, J = 4.0, 5.4 Hz, 1 H), 7.67 (dd, J = 5.8, 5.9 Hz, 1 H), 4.21 (s, 2 H, CH_2) ppm.

Ligand 1: Sodium iodide (1.2 equiv., 0.94 g; 0.63 mmol) was added to **4** (0.166 g, 0.63 mmol) dissolved in dry acetonitrile (20 mL) (pale yellow solution). The solution was stirred for 10 min at room temperature until a white precipitate appeared (NaBr). Next, 30% methylamine solution in ethanol (5 mL) was added in portions over 6 h of stirring at room temperature until analysis by TLC indicated no starting compound was present. The reaction mixture was evaporated under reduced pressure and was further purified by silica column chromatography using 95:5 CH_2Cl_2/MeOH(NH_3) as eluent to give a yellow-brown solid (0.126 g, 90%). ^{1}H NMR (400 MHz, $CDCl_3$, 298 K): δ = 10.23 (br. s, 1 H, NH), 9.26 (d, J = 4.0 Hz, 1 H), 9.14 (d, J = 4.0 Hz, 1 H), 8.65 (s, 1 H), 8.34 (d, J = 8.4 Hz, 1 H), 8.26 (d, J = 8.0 Hz, 1 H), 7.73 (dd, J = 4.3, 4.3 Hz, 1 H), 7.67 (dd, J = 4.3, 4.3 Hz, 1 H), 3.58 (s, 2 H, CH_2), 2.68 (s, 3 H, CH_3) ppm. ^{13}C NMR (100 MHz, $CDCl_3$, 298 K): δ = 170.2, 150.2, 149.6, 135.9, 130.2, 128.7, 123.5, 123.2, 122.8, 116.6, 55.4, 37.2 ppm. HRMS: calcd. for $C_{15}H_{15}N_4O$ [M + H] 267.12; found 267.2.

Tiiii-C: Dichlorophenylphosphine (0.081 mL, 0.582 mmol) was added slowly at room temperature to a solution of heptadecyl-footed resorcinarene (130 mg, 0.090 mmol) in freshly distilled pyridine (10 mL). After 3 h of stirring at 70 °C, the solution was cooled to room temperature and aqueous 35% H_2O_2 (2 mL) was added. The resulting mixture was stirred for 30 min at room temperature. H_2O (100 mL) was added and the solution was filtered. The solid was suspended in water (100 mL), sonicated for 30 min and filtered again resulting in a white powder (140 mg, 80%). ^{1}H NMR (400 MHz, $CDCl_3$): δ = 8.10–8.04 (m, 8 H, PO–Ar–H_o), 7.64 (m, 4 H, POArH$_p$), 7.55–7.51 (m, 8 H, POArH$_m$), 7.31 (s, 4 H, Ar–H$_{up}$), 7.02 (s, 4 H, Ar–H$_{down}$), 4.82 (bt, 4 H, Ar–CH–Ar), 2.36 (bd, 8 H, –CH–CH_2–CH_2–), 1.47 (m, 8 H, –CH_2–CH_2–CH_3), 1.28 [m, 112 H, –CH_2–$(CH_2)_{14}$–CH_3], 0.90 (m, 12 H, –CH_2–CH_3) ppm. ^{31}P NMR (160 MHz, $CDCl_3$): δ = 7.6 (s, 4 P) ppm.

Cavitand–Guest–Ligand Complex Tiiii-A·1: A solution of CH_3COCl in methanol (0.752 M, 0.1 mL used) was added dropwise to a solution of **1** in methanol (20 mg, 0.0752 mmol). Cavitand Tiiii-**A** (89 mg, 0.0752 mmol) was added to this transparent solution. The mixture was stirred until everything dissolved (5 min, room temp.). Next, the solvent was removed under reduced pressure and an orangish residue, Tiiii-**A**·**1**, was dried under vacuum. ^1H NMR (400 MHz, $CDCl_3$, 298 K): for **1**: δ = 9.34 (br. s, 1 H), 9.26 (br. s, 1 H), 9.02 (br. s, 1 H), 8.43 (br. s, 1 H), 7.80 (s, 1 H), 7.71 (s, 1 H), 7.30 (br. s, 1 H), 6.83 (br. s, 2 H, NH_2) 3.76 (s, 2 H, CH_2), –0.50 (s, 3 H, CH_3) ppm; for Tiiii-**A**: δ = 8.15 (q, J = 7.2 Hz, 8 H, Ar–H), 7.82 (br. s, 4 H, Ar–H), 7.73 (t, J = 7.6 Hz, 4 H, Ar–H), 7.60 (m, 8 H, Ar–H), 4.83 (t, J = 7.6 Hz, 4 H, Ar–*CH*–Ar), 2.63 (m, 8 H, $CH{-}\mathit{CH_2}{-}CH_2$), 2.20 (s, 12 H, $Ar{-}CH_3$), 1.46 (m, 8 H, $CH_2{-}\mathit{CH_2}{-}CH_3$), 1.10 (m, 12 H, $CH_2{-}\mathit{CH_3}$) ppm. ^{31}P NMR (160 MHz, $CDCl_3$, 298 K): δ = 10.8 (s, 4 P) ppm.

Tiiii-C·1: A solution of CH_3COCl in methanol (0.403 M, 0.1 mL used) was added dropwise to a solution of **1** in methanol (11 mg, 0.040 mmol). Cavitand Tiiii-**C** (78 mg, 0.040 mmol) was added to this transparent solution. The mixture was stirred for 5 min at room temperature. The resulting orangish residue was dried under vacuum. ^1H NMR (400 MHz, $CDCl_3$, 298 K): for **1**: δ = 9.30 (br. s, 2 H), 9.02 (br. s, 1 H), 8.49 (m, 4 H), 3.80 (s, 2 H, CH_2), –0.64 (s, 3 H, CH_3) ppm; for Tiiii-**C**: δ = 8.10 (m, 8 H, PO–Ar–H), 7.69 (m, 4 H, PO–Ar–H), 7.58 (m, 8 H, PO–Ar–H), 7.25 (br. s, 4 H, Ar–H), 6.97 (br. s, 4 H, Ar–H), 4.78 (t, J = 6.6 Hz, 4 H, Ar–*CH*–Ar), 2.85 (br. s, 8 H, $CH{-}\mathit{CH_2}{-}CH_2$), 1.51 (br. s, 8 H, $CH{-}CH_2{-}\mathit{CH_2}$), 1.42 [m, 112 H, $CH_2{-}(\mathit{CH_2})_{14}{-}CH_3$], 0.89 (m, 12 H, $CH_2{-}CH_2{-}\mathit{CH_3}$) ppm. ^{31}P NMR (160 MHz, $CDCl_3$, 298 K): δ = 12.1 (s, 4 P) ppm.

Ternary Complex Tiiii-**A**·**1**·**2:** Complex **2** (14 mg, 0.017 mmol) was added at once to a solution of Tiiii-**A**·**1** in dichloromethane (25 mg, 0.017 mmol) and the mixture was stirred for 1 h at room temperature. The solvent was removed under reduced pressure and orange residue Tiiii-**A**·**1**·**2** was dried under vacuum. ^{31}P NMR (160 MHz, $CDCl_3$, 298 K): δ = 11.3 (s, 4 P) ppm.

Ternary Complex Tiiii-A·1·3: Complex **3** (14.2 mg, 0.02 mmol) was added at once to a solution of Tiiii-**A**·**1** in dichloromethane (30 mg, 0.02 mmol) and the mixture was stirred for 1 h at room temperature. The solvent was removed under reduced pressure and orange residue Tiiii-**A**·**1**·**3** was dried under vacuum. ^1H NMR (400 MHz, $CDCl_3$): for **1**: δ = 9.25 (br. s, 1 H), 9.18 (br. s, 1 H), 8.70 (br. s, 1 H), 8.46 (s, 1 H), 8.23 (br. s, 1 H), 7.70 (br. s, 1 H), 7.09 (br. s, 1 H), 6.83 (br. s, 2 H, NH_2), 3.58 (br. s, 2 H, CH_2), –0.58 (s, 3 H, CH_3); for **2**: δ = 6.07 (br. s, 2 H), 6.00 (br. s, 1 H) ppm; for Tiiii-**A**: δ = 8.10 (q, J = 7.2 Hz, 8 H, Ar–H), 7.82 (br. s, 4 H, Ar–H), 7.75 (t, J = 7.04 Hz, 4 H, Ar–H), 7.59 (m, 8 H, Ar–H), 4.83 (t, J = 7.2 Hz, 4 H, Ar–*CH*–Ar), 2.61 (m, 8 H, $CH{-}\mathit{CH_2}{-}CH_2$), 2.18 (s, 12 H, $Ar{-}CH_3$), 1.47 (m, 8 H, $CH_2{-}\mathit{CH_2}{-}CH_3$), 1.10 (m, 12 H, $CH_2{-}\mathit{CH_3}$) ppm. ^{31}P NMR (160 MHz, $CDCl_3$, 298 K): δ = 11.0 (s, 4 P) ppm.

Ternary Complex Tiiii-C·1·2: Tiiii-**C**·**1** (29 mg, 0.013 mmol) and [Eu(hfac)$_3$] (10.5 mg, 0.013 mmol) were dissolved in dichloromethane (10 mL) and the solution was stirred for 1 h at room temperature until everything was dissolved. The solvent was removed under reduced pressure and the residue was dried under vacuum. ^{31}P NMR (160 MHz, $CDCl_3$, 298 K): δ = 12.6 (s, 4 P) ppm. HRMS: calcd. for $[M - Cl]^+$ $C_{150}H_{190}EuF_{18}N_4O_{19}P_4^+$ 2971.19277; found 2971.18155.

Synthesis of Si-Tiiii-B: The Tiiii-**B**/1-octene mixture (χ_{cav} = 0.05) was dissolved in mesitylene (solution concentration = 50 mM) and this solution (2.0 mL) was placed in a quartz cell and deoxygenated by stirring in a dry box for at least 1 h. A Si(100) substrate was dipped in H_2SO_4/H_2O_2 (3:1) solution for 12 min to remove organic contaminants, then it was etched in a hydrofluoric acid solution (1% v/v) for 90 s and quickly rinsed with water. The resulting hydrogenated silicon substrate was immediately placed in the above-mentioned mesitylene solution. The cell remained under UV irradiation (254 nm) for 2 h. The sample was then removed from the solution and was sonicated twice in dichloromethane for 10 min to remove residual physisorbed material.

Host–Guest System on Silicon (Si-Tiiii-B·1): A Si-Tiiii-**B** wafer was dipped in a 1×10^{-3} M solution of guest **1** in CH_3OH for 60 min, sonicated in CH_3OH for 5 min and dried in nitrogen flux.

Ternary Complex on Silicon with 2 and 3, Si-Tiiii-B·1·2 and Si-Tiiii-B·1·3: Si-Tiiii-**B**·**1** was dipped in solutions of complexes **2** and **3** in THF (1×10^{-3} M) for 30 min, sonicated in THF for 5 min and dried in nitrogen flux.

Photophysical Measurements: Absorption spectra were recorded in Hellma quartz cells (1 cm) with a Perkin–Elmer Lambda 950 UV/Vis/NIR spectrophotometer. Steady-state photoluminescence spectra and excitation spectra were recorded with an Edinburgh FLS920 spectrometer (continuous 450 W Xe lamp), equipped with a Peltier-cooled Hamamatsu R928 photomultiplier tube (185–850 nm). Emission quantum yields of Eu^{III}-based samples were determined according to the approach described by Demas and Crosby[25] by using [Ru(bipy)$_3$Cl$_2$] (Φ_{em} = 0.028 in air-equilibrated water solution; bipy = 2,2′-bipyridine)[26] as standard.

Excited-state lifetimes on the nanosecond timescale were measured with a IBH 5000F time-correlated single-photon-counting spectrometer, by using pulsed NanoLED excitation sources at 278 nm; analysis of the luminescence decay profiles was done with Decay Analysis Software DAS6 provided by the manufacturer. Emission decays on the millisecond timescale were measured with a Perkin–Elmer LS-50B spectrofluorimeter equipped with a pulsed Xe lamp and in gated detection mode. The phosphorescence decay analysis was performed with the PHOSDecay software provided by the manufacturer. Experimental uncertainties are estimated to be ±2 and ±5 nm for absorption and emission peaks, ±20% for emission quantum yields, and ±8% for lifetimes.

Supporting Information (see footnote on the first page of this article): It contains the monitoring data for the formation of complexes by means of ^1H and ^{31}P NMR spectroscopy; the HRMS spectrum of the ternary complex; absorption spectra; XPS data; and competition experiments.

Acknowledgments

This work was supported by the European Union (contract PITN-GA-2008-215399 - FINELUMEN). The authors also thank MIUR for partial financial support through FIRB "RINAME" (RBAP114AMK). The authors thank Dr. Nicola Armaroli of Molecular Photoscience Group, Istituto per la Sintesi Organica e la Fotoreattività del CNR (ISOF-CNR) for support with the photophysical measurements and for fruitful discussion of the results. J. M. M. further thanks Istituto di Studi Avanzati, University of Bologna, for the BRAINS-IN fellowship. Centro Interdipartimentale Misure "G. Casnati" of the University of Parma is acknowledged for the use of NMR spectroscopy and HR ESI-MS facilities. [Eu(hfac)$_3$] was kindly provided by Prof. Marek Pietraszkiewicz of the Institute of Physical Chemistry of the Polish Academy of Science, Warsaw.

---

[1] W. A. Lopes, H. M. Jaeger, *Nature* **2001**, *414*, 735–738.
[2] J. Paczesny, A. Kamińska, W. Adamkiewicz, K. Winkler, K. Sozanski, M. Wadowska, I. Dziecielewski, R. Holyst, *Chem. Mater.* **2012**, *24*, 3667–3673.
[3] M. J. W. Ludden, D. N. Reinhoudt, J. Huskens, *Chem. Soc. Rev.* **2006**, *35*, 1122–1134.

[4] A. B. Descalzo, R. Martinez-Máñez, F. Sancenón, K. Hoffmann, K. Rurack, *Angew. Chem. Int. Ed.* **2006**, *45*, 5924–5948; *Angew. Chem.* **2006**, *118*, 6068.

[5] D. J. Cram, J. M. Cram, *Container Molecules and Their Guests* (Ed.: J. F. Stoddart), The Royal Society of Chemistry, Cambridge, UK, **1994**.

[6] a) D. M. Rudkevich, J. Rebek Jr., *Eur. J. Org. Chem.* **1999**, *9*, 1991–2005; b) H.-J. Choi, Y.-S. Park, J. Song, S. J. Youn, H.-S. Kim, S.-H. Kim, K. Koh, K. Paek, *J. Org. Chem.* **2005**, *70*, 5974–5981; c) T. Gottschalk, B. Jaun, F. Diederich, *Angew. Chem. Int. Ed.* **2007**, *46*, 260–264; *Angew. Chem.* **2007**, *119*, 264; d) S. M. Biros, J. Rebek Jr., *Chem. Soc. Rev.* **2007**, *36*, 93–104; e) M. Nikan, J. C. Sherman, *J. Org. Chem.* **2009**, *74*, 5211–5218; f) D. Ajami, J. Rebek Jr., *Nat. Chem.* **2009**, *1*, 87–90; g) S. M. Grayson, B. C. Gibb, *Soft Matter* **2010**, *6*, 1377–1382; h) S. Liu, H. Gan, A. T. Hermann, S. W. Rick, B. C. Gibb, *Nat. Chem.* **2010**, *2*, 847–852; i) F. Maffei, P. Betti, D. Genovese, M. Montalti, L. Prodi, R. De Zorzi, S. Geremia, E. Dalcanale, *Angew. Chem. Int. Ed.* **2011**, *50*, 4654–4657; *Angew. Chem.* **2011**, *123*, 4750; j) J. Hornung, D. Fankhauser, L. D. Shirtcliff, A. Praetorius, W. B. Schweizer, F. Diederich, *Chem. Eur. J.* **2011**, *17*, 12362–12371; k) J. Vachon, S. Harthong, E. Jeanneau, C. Aronica, N. Vanthuyne, C. Roussel, J.-P. Dutasta, *Org. Biomol. Chem.* **2011**, *9*, 5086–5091.

[7] F. Tancini, D. Genovese, M. Montalti, L. Cristofolini, L. Nasi, L. Prodi, E. Dalcanale, *J. Am. Chem. Soc.* **2010**, *132*, 4781–4789.

[8] E. Menozzi, R. Pinalli, E. A. Speets, B. J. Ravoo, E. Dalcanale, D. N. Reinhoudt, *Chem. Eur. J.* **2004**, *10*, 2199–2206; M. Dionisio, F. Maffei, E. Rampazzo L. Prodi, A. Pucci, G. Ruggeri, E. Dalcanale, *Chem. Commun.* **2011**, *47*, 6596–6598.

[9] a) M. Busi, M. Laurenti, G. G. Condorelli, A. Motta, M. Favazza, I. L. Fragala, M. Montalti, L. Prodi, E. Dalcanale, *Chem. Eur. J.* **2007**, *13*, 6891–6898; b) E. Biavardi, M. Favazza, A. Motta, I. L. Fragalà, C. Massera, L. Prodi, M. Montalti, M. Melegari, G. G. Condorelli, E. Dalcanale, *J. Am. Chem. Soc.* **2009**, *131*, 7447–7455; c) C. Tudisco, P. Betti, A. Motta, R. Pinalli, L. Bombaci, E. Dalcanale, G. G. Condorelli, *Langmuir* **2012**, *28*, 1782–1789.

[10] a) S. H. Hsu, M. D. Yilmaz, C. Blum, V. Subramaniam, D. N. Reinhoudt, A. H. Velders, J. Huskens, *J. Am. Chem. Soc.* **2009**, *131*, 12567–12569; b) M. D. Yilmaz, S. H. Hsu, D. N. Reinhoudt, A. H. Velders, J. Huskens, *Angew. Chem. Int. Ed.* **2010**, *49*, 5938–5941; *Angew. Chem.* **2010**, *122*, 6074; c) S. H. Hsu, M. D. Yilmaz, D. N. Reinhoudt, A. H. Velders, J. Huskens, *Angew. Chem. Int. Ed.* **2013**, *52*, 714–719.

[11] a) S. V. Eliseeva, J. C. G. Bünzli, *Chem. Soc. Rev.* **2010**, *39*, 189–227; b) K. Binnemans, *Chem. Rev.* **2009**, *109*, 4283–4374.

[12] J.-C. G. Bünzli, A.-S. Chauvin, H. K. Kim, E. Deiters, S. V. Eliseeva, *Coord. Chem. Rev.* **2010**, *254*, 2623–2633.

[13] a) J.-C. G. Bünzli, *Chem. Rev.* **2010**, *110*, 2729; b) S. V. Eliseeva, J.-C. G. Bünzli, *New J. Chem.* **2011**, *35*, 1165–1176.

[14] A. M. Nonat, A. J. Harte, K. Sénéchal-David, J. P. Leonard, T. Gunnlaugsson, *Dalton Trans.* **2009**, 4703–4711.

[15] G. G. Condorelli, C. Tudisco, A. Di Mauro, F. Lupo, A. Gulino, A. Motta, I. L. Fragalà, *Eur. J. Inorg. Chem.* **2010**, 4121–4129.

[16] A. Gulino, F. Lupo, G. G. Condorelli, A. Motta, I. Fragalà, *J. Mater. Chem.* **2009**, *19*, 3507–3511.

[17] E. Biavardi, C. Tudisco, F. Maffei, A. Motta, C. Massera, G. G. Condorelli, E. Dalcanale, *Proc. Natl. Acad. Sci. USA* **2012**, *109*, 2263–2268.

[18] G. Accorsi, A. Listorti, K. Yoosaf, N. Armaroli, *Chem. Soc. Rev.* **2009**, *38*, 1690–1700.

[19] A. Bencini, V. Lippolis, *Coord. Chem. Rev.* **2010**, *254*, 2096–2180.

[20] For the nomenclature adopted for phosphonate cavitands, see: R. Pinalli, M. Suman, E. Dalcanale, *Eur. J. Org. Chem.* **2004**, 451–462.

[21] G. G. Condorelli, A. Motta, M. Favazza, I. L. Fragalà, M. Busi, E. Menozzi, E. Dalcanale, *Langmuir* **2006**, *22*, 11126–11133.

[22] J. Qi, T. Matsumoto, M. Tanaka, Y. Masumoto, *J. Phys. D* **2000**, *22*, 2074–2078.

[23] E. Biavardi, G. Battistini, M. Montalti, R. M. Yebeutchou, L. Prodi, E. Dalcanale, *Chem. Commun.* **2008**, 1638–1640.

[24] B. Bibal, B. Tinant, J.-P. Declercq, J.-P. Dutasta, *Supramol. Chem.* **2003**, *15*, 25–32.

[25] J. N. Demas, G. A. Crosby, *J. Phys. Chem.* **1971**, *75*, 991–1024.

[26] K. Nakamaru, *Bull. Chem. Soc. Jpn.* **1982**, *55*, 2697–2705.

Received: February 27, 2014
Published Online: April 30, 2014